

Singularity-free dark energy star

Farook Rahaman* and Raju Maulick†

Department of Mathematics, Jadavpur University, Kolkata 700 032, West Bengal, India

Anil Kumar Yadav‡

Department of Physics, Anand Engineering College, Keetham, Agra -282 007, India

Saibal Ray§

Department of Physics, Government College of Engineering & Ceramic Thechnology, Kolkata 700 010, West Bengal, India

Ranjan Sharma¶

Department of Physics, P. D. Women's College, Jalpaiguri 735101, India.

(Dated: January 12, 2013)

We propose a model for an anisotropic dark energy star where we assume that the radial pressure exerted on the system due to the presence of dark energy is proportional to the isotropic perfect fluid matter density. We discuss various physical features of our model and show that the model satisfies all the regularity conditions and is stable as well as singularity-free.

PACS numbers: 04.40.Nr, 04.20.Jb, 04.20.Dw

I. INTRODUCTION

Current cosmological observations of the accelerated expansion of the universe strongly suggest that about 96% of the total energy content of the universe is exotic in nature out of which 73% is believed to be gravitationally repulsive in nature popularly called *dark energy* and the remaining 23% is attractive in nature and exists in the form of dark matter [1, 2]. Consequently, cosmological models based on dark energy either in the form of a cosmological constant or in some other exotic forms of matter have got tremendous attention in the recent past. From the astrophysical perspective, if it is fundamentally impossible to get any observational evidence for the existence of an event horizon in our universe [3] (though our current understanding of the general theory of relativity strongly favour the existence of strong gravitational regions induced by compact objects covered under the event horizon), one is tempted to look for alternative models which may serve as alternatives to black holes. A dark energy star is, in particular, interesting in this scenario [4].

Any interior solution to the vacuum Schwarzschild exterior comprising a fluid distribution governed by an equation of state(EOS) of the form $p = -\frac{1}{3}\rho$, may be considered as a dark energy star [5]. In the past, various model specific dark energy stars have been proposed (see for example, Ref. [4–8] and Ref. [9] for a recent review). In the present work, we propose a model for an

anisotropic dark energy star where we assume that the radial pressure exerted on the system due to the presence of dark energy is proportional to the isotropic perfect fluid matter density. The stellar configuration comprises two fluids - an ordinary baryonic perfect fluid together with an yet unknown form of matter (dark energy) which is repulsive in nature. We also assume that the two fluids are non interacting amongst each other.

To describe the energy-momentum tensor for such a hybrid model, we assume that our resulting composition is anisotropic in nature, i.e. $p_r \neq p_t$, where p_r and p_t correspond to radial and tangential pressure, respectively. Ever since the pioneering works of Bowers and Liang [10], anisotropic relativistic stellar models have played an important role in the description of compact stellar objects (see [11] for a recent review). At the microscopic level, a variety of reasons such as the existence of type 3A superfluid, phase transition, pion condensation, rotation, magnetic field, mixture of two fluids, bosonic composition etc., may give rise to anisotropic pressures inside a stellar object. Recent observations on highly compact astrophysical objects like X ray pulsar Her X-1, X ray buster 4U 1820-30, millisecond pulsar SAX J 1808.4 - 3658, X ray sources 4U 1728 - 34, etc., also strongly favour an anisotropic matter distribution since the density inside such an ultra-compact object is expected to be beyond nuclear matter density. In our model, we assume that the anisotropy is generated due to two kinds of fluid distributions. In a recent paper [12], an exterior solution corresponding to a two fluid stellar model composed of non-interacting phantom scalar field describing the dark energy and ordinary matter has been reported which reduces to Schwarzschild solution in the absence of the dark energy. In our paper, we match the interior solution to the Schwarzschild exterior solution at the boundary.

Our paper is organized as follows: In Section II we have provided the basic equations in connection to the

*Electronic address: farook_rahaman@yahoo.com

†Electronic address: rajuspinor@gmail.com

‡Electronic address: abanilyadav@yahoo.co.in

§Electronic address: saibal@iucaa.ernet.in

¶Electronic address: rsharma@iucaa.ernet.in

proposed model for dark energy star. Sections. III - VIII are dealt, respectively, with the boundary conditions, TOV equation, energy conditions, stability, mass-radius relation and junction conditions for the solutions under consideration. Some concluding remarks are made in the Section IX.

II. BASIC EQUATIONS AND THEIR SOLUTIONS

To describe the space-time of the dark energy stellar configuration, we take the Krori and Barua [13] metric (henceforth KB) given by

$$ds^2 = -e^{\nu(r)} dt^2 + e^{\lambda(r)} dr^2 + r^2(d\theta^2 + \sin^2\theta d\phi^2), \quad (1)$$

with $\lambda(r) = Ar^2$ and $\nu(r) = Br^2 + C$ where A , B and C are arbitrary constants to be determined on physical grounds. The energy-momentum of the two fluids are such that

$$T_0^0 \equiv (\rho)_{eff} = \rho + \rho_{de}, \quad (2)$$

$$T_1^1 \equiv -(p_r)_{eff} = -(p + p_{der}), \quad (3)$$

$$T_2^2 \equiv T_3^3 \equiv -(p_t)_{eff} = -(p + p_{det}), \quad (4)$$

where ρ and p correspond to the energy density and pressure of the baryonic matter, respectively, and ρ_{de} , p_{der} and p_{det} are the ‘dark’ energy density, radial pressure and tangential pressure, respectively. The left hand sides of equations (2)-(4) are the effective energy-density and two pressures, respectively, of the composition.

The Einstein’s field equations for the metric (1) are then obtained as (we assume $G = c = 1$ under geometrized relativistic units)

$$8\pi(\rho + \rho_{de}) = e^{-\lambda} \left(\frac{\lambda'}{r} - \frac{1}{r^2} \right) + \frac{1}{r^2}, \quad (5)$$

$$8\pi(p + p_{der}) = e^{-\lambda} \left(\frac{\nu'}{r} + \frac{1}{r^2} \right) - \frac{1}{r^2}, \quad (6)$$

$$8\pi(p + p_{det}) = \frac{e^{-\lambda}}{2} \left[\frac{\nu'^2 - \lambda'\nu'}{2} + \frac{\nu' - \lambda'}{r} + \nu'' \right]. \quad (7)$$

To solve the above set of equations, we assume that the dark energy radial pressure is proportional to the dark energy density, i.e.,

$$p_{der} = -\rho_{de}, \quad (8)$$

and the dark energy density is proportional to the matter density, i.e.,

$$\rho_{de} = \alpha\rho, \quad (9)$$

where $\alpha > 0$ is a proportionality constant. In connection to the *ansatz* (8) it is worthwhile to mention that the equation of state of this type which implies that the matter distribution under consideration is in tension is

available in literature and hence the matter is known as a ‘false vacuum’ or ‘degenerate vacuum’ or ‘ ρ -vacuum’ [14–17].

Now, from the metric (1) we get $\lambda' = 2Ar$, $\nu' = 2Br$ and $e^{-\lambda} = e^{-Ar^2}$ and substituting these values in equations (5) - (7), together with our assumptions as given in equations (8) and (9), we get

$$8\pi\rho = \frac{1}{(1+\alpha)} \left[e^{-Ar^2} \left(2A - \frac{1}{r^2} \right) + \frac{1}{r^2} \right], \quad (10)$$

$$8\pi(\rho + p) = 2e^{-Ar^2} (A + B). \quad (11)$$

Subtracting equation (10) from (11), we get

$$8\pi p = e^{-Ar^2} (2A + 2B) - \frac{1}{(1+\alpha)} \left[e^{-Ar^2} \left(2A - \frac{1}{r^2} \right) + \frac{1}{r^2} \right]. \quad (12)$$

The equation (12), alongwith (7), then provides

$$8\pi p_{det} = e^{-Ar^2} [B^2r^2 - AB r^2 - 3A] + \frac{1}{(1+\alpha)} \left[e^{-Ar^2} \left(2A - \frac{1}{r^2} \right) + \frac{1}{r^2} \right]. \quad (13)$$

Thus the effective energy density $(\rho)_{eff}$, effective radial pressure $(p_r)_{eff}$ and the effective tangential pressure $(p_t)_{eff}$ are obtained as

$$(\rho)_{eff} = \frac{1}{8\pi} \left[e^{-Ar^2} \left(2A - \frac{1}{r^2} \right) + \frac{1}{r^2} \right], \quad (14)$$

$$(p_r)_{eff} = \frac{1}{8\pi} \left[e^{-Ar^2} \left(2B + \frac{1}{r^2} \right) - \frac{1}{r^2} \right], \quad (15)$$

$$(p_t)_{eff} = \frac{1}{8\pi} \left[e^{-Ar^2} (B^2r^2 + 2B - AB r^2 - A) \right] \quad (16)$$

Using equations (16) - (18) the equation of state (EOS) corresponding to radial and transverse directions may be written as

$$\omega_r(r) = \frac{[e^{-Ar^2} (2B + \frac{1}{r^2}) - \frac{1}{r^2}]}{[e^{-Ar^2} (2A - \frac{1}{r^2}) + \frac{1}{r^2}]} \quad (17)$$

$$\omega_t(r) = \frac{[e^{-Ar^2} (B^2r^2 + 2B - AB r^2 - A)]}{[e^{-Ar^2} (2A - \frac{1}{r^2}) + \frac{1}{r^2}]} \quad (18)$$

It is interesting to note that the effective energy density (ρ_{eff}) , effective radial pressure $(p_r)_{eff}$ and effective tangential pressure $(p_t)_{eff}$ are independent of α .

We also note that

$$\frac{d\rho_{eff}}{dr} = -\frac{1}{8\pi} \left[\left(4A^2r - \frac{2A}{r} - \frac{2}{r^3} \right) e^{-Ar^2} + \frac{2}{r^3} \right] < 0,$$

and

$$\frac{dp_{r\,eff}}{dr} < 0.$$

We impose the following conditions for our anisotropic fluid configuration to be physically acceptable:

- The density is positive definite and its gradient is negative everywhere within the fluid distribution.
- The radial and tangential pressures are positive definite and the radial pressure gradient is negative definite.

The above results and Figs. 1-2 are in agreement with these conditions.

Note that, at $r = 0$, our model provides

$$\frac{d\rho_{eff}}{dr} = 0, \quad \frac{dp_{r\ eff}}{dr} = 0,$$

$$\frac{d^2\rho_{eff}}{dr^2} = -\frac{A^2}{\pi} < 0,$$

and

$$\frac{d^2p_{r\ eff}}{dr^2} < 0,$$

which indicate maximality of central density and central pressure. Interestingly, similar to an ordinary matter distribution, the bound on the effective EOS in this construction is given by $0 < \omega_i(r) < 1$, (see Fig. 3) despite the fact that star is constituted by the combination of ordinary matter and dark energy.

The parameter $\Delta = \frac{2}{r}(p_{t\ eff} - p_{r\ eff})$ representing the ‘force’ due to the local anisotropy is obtained as

$$\Delta = \frac{1}{4\pi r} \left[e^{-Ar^2} (B^2 r^2 - AB r^2 - 3A) \right] + \frac{1}{8\pi} \left[e^{-Ar^2} \left(2A - \frac{1}{r^2} \right) + \frac{1}{r^2} \right]. \quad (19)$$

This ‘force’ will be directed outward when $P_t > P_r$ i.e. $\Delta > 0$, and inward if $P_t < P_r$ i.e. $\Delta < 0$. As it is apparent from the Fig. 4 of our model with a repulsive ‘anisotropic’ force ($\Delta > 0$) allows the construction of more massive distributions.

III. BOUNDARY CONDITIONS

We match the interior metric to the Schwarzschild exterior

$$ds^2 = - \left(1 - \frac{2M}{r} \right) dt^2 + \left(1 - \frac{2M}{r} \right)^{-1} dr^2 + r^2 (d\theta^2 + \sin^2 \theta d\phi^2), \quad (20)$$

at the boundary $r = R$. Assuming continuity of the metric functions g_{tt} , g_{rr} and $\frac{\partial g_{tt}}{\partial r}$ at the boundary surface S , we get

$$1 - \frac{2M}{R} = e^{BR^2+C}, \quad (21)$$

$$\left(1 - \frac{2M}{R} \right)^{-1} = e^{AR^2}, \quad (22)$$

$$\frac{M}{R^2} = BR e^{BR^2+C}. \quad (23)$$

By solving Eqs. (21)-(23), we have

$$A = -\frac{1}{R^2} \ln \left[1 - \frac{2M}{R} \right], \quad (24)$$

$$B = \frac{1}{R^2} \left[\frac{M}{R} \right] \left[1 - \frac{2M}{R} \right]^{-1}, \quad (25)$$

$$C = \ln \left[1 - \frac{2M}{R} \right] - \frac{\frac{M}{R}}{\left[1 - \frac{2M}{R} \right]}. \quad (26)$$

We also impose the boundary conditions that at the boundary $(p_r)_{eff}(r = R) = 0$ and $\rho_{eff}(r = 0) = b$ ($= a$ constant), where b is the central density. Thus,

$$A = \frac{8\pi b}{3}, \quad (27)$$

$$B = \frac{1}{2R^2} \left[e^{\frac{8\pi b}{3} R^2} - 1 \right]. \quad (28)$$

Combining, equations (24) and (27), we get

$$A = \frac{8\pi b}{3} = -\frac{1}{R^2} \ln \left[1 - \frac{2M}{R} \right]. \quad (29)$$

Note that the values of B obtained from equations (25) and (28) are identical.

At this juncture, to get an insight of our model, let us first evaluate some reasonable set for values of A , B , and C . According to Buchdahl [18], the maximum allowable compactness (mass-radius ratio) for a fluid sphere is given by $\frac{2M}{R} < \frac{8}{9}$. Accordingly, let us assume that we have a dark energy star whose mass and radius are such that $\frac{M}{R} = 0.3999052$. Due to highly compact nature of the star, we set the radius of the star at $R = 8$ km. With these specifications, we obtain the values of the constants A , B and b as $A = .025$, $B = .030883$, $b = .002984$. Later, we have shown that these values of A and B are justified since the energy conditions imply $2A \geq B \geq 0$ (see Sec. V).

IV. TOV EQUATION

For an anisotropic fluid distribution, the generalized TOV equation is given by

$$\frac{d(p_{r\ eff})}{dr} + \nu' (\rho_{eff} + p_{r\ eff}) + \frac{2}{r} (p_{r\ eff} - p_{t\ eff}) = 0. \quad (30)$$

Following Ponce de León [19], we write the above TOV equation as

$$- \frac{M_G (\rho_{eff} + p_{r\ eff})}{r^2} e^{\frac{\lambda-\nu}{2}} - \frac{dp_{r\ eff}}{dr} + \frac{2}{r} (p_{t\ eff} - p_{r\ eff}) = 0, \quad (31)$$

where $M_G = M_G(r)$ is the effective gravitational mass inside a sphere of radius r and is given by

$$M_G(r) = \frac{1}{2} r^2 e^{\frac{\nu-\lambda}{2}} \nu', \quad (32)$$

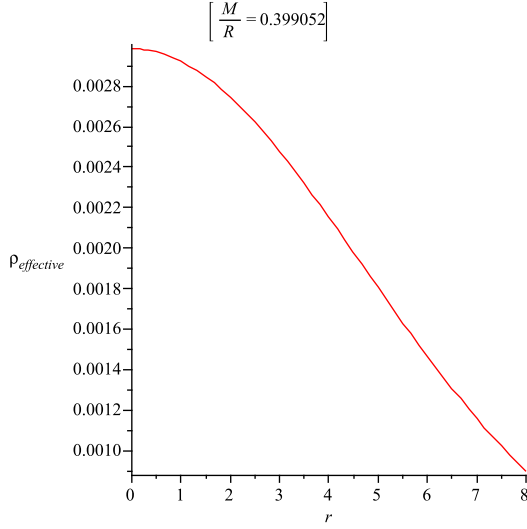


FIG. 1: The effective density parameter ρ_{eff} is shown against r .

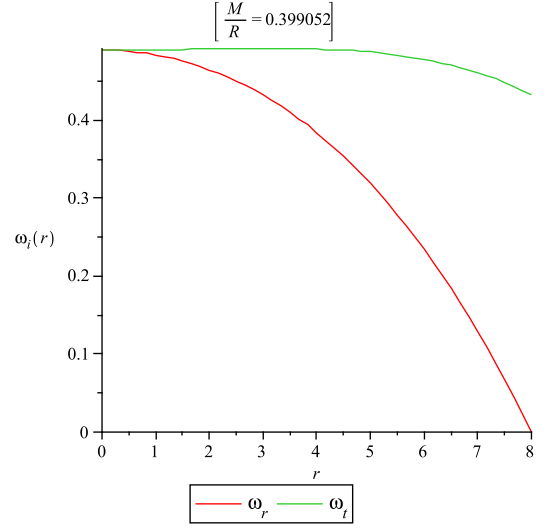


FIG. 3: The variation of the effective equation of state parameter ω (radial and transverse) are shown against r .

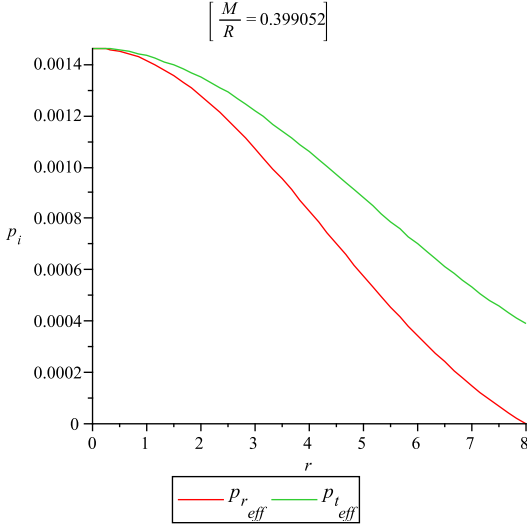


FIG. 2: Effective radial pressure and transverse pressures are plotted against r .

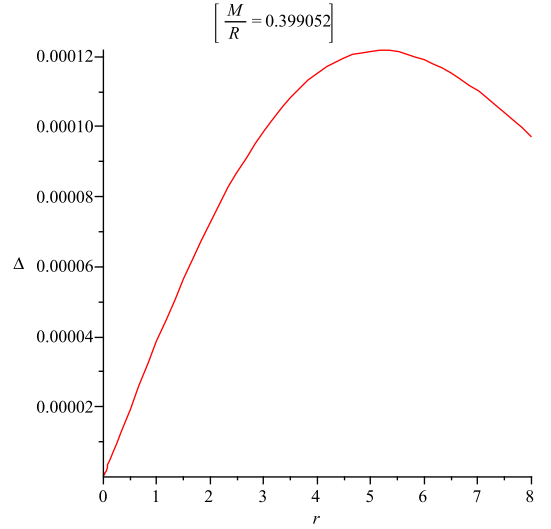


FIG. 4: The variation of the force, $\Delta = \frac{2}{r} (p_{t\,eff} - p_{r\,eff})$ due to the local anisotropy with respect to r .

which can easily be derived from the Tolman-Whittaker formula and the Einstein's field equations. Obviously, the modified TOV equation describes the equilibrium condition for the dark star subject to gravitational and hydrostatic plus another force due to the anisotropic nature of the stellar object. Using equations (14) - (16), the above equation can be written as

$$F_g + F_h + F_a = 0, \quad (33)$$

where,

$$F_g = -Br(\rho_{eff} + p_{r\,eff}), \quad (34)$$

$$F_h = -\frac{dp_{r\,eff}}{dr}, \quad (35)$$

$$F_a = \frac{2}{r}(p_{t\,eff} - p_{r\,eff}). \quad (36)$$

The profiles of F_g , F_h and F_a for our chosen source are shown in Fig. 5. The figure indicates that the static equilibrium is attainable due to pressure anisotropy, gravitational and hydrostatic forces.

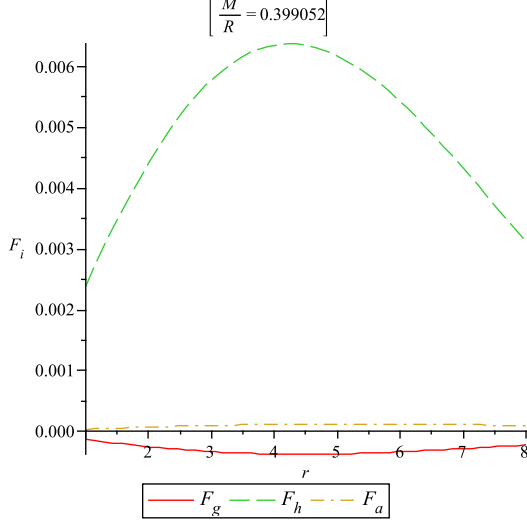


FIG. 5: Three different forces acting on fluid elements in static equilibrium is shown against r .

V. ENERGY CONDITIONS

In this section, we verify whether our particular choices of the values of mass and radius leading to solutions for the unknown parameters, satisfy the following conditions through out the configuration:

$$\rho_{eff} \geq 0,$$

$$\rho_{eff} + p_{r\,eff} \geq 0,$$

$$\rho_{eff} + p_{t\,eff} \geq 0,$$

$$\rho_{eff} + p_{r\,eff} + 2p_{t\,eff} \geq 0,$$

$$\rho_{eff} > |p_{r\,eff}|,$$

$$\rho_{eff} > |p_{t\,eff}|.$$

Note that all the energy conditions namely, the null energy condition (NEC), weak energy condition (WEC), strong energy condition (SEC) and dominant energy condition (DEC), for our particular choices of the values of mass and radius, are satisfied as shown in Fig. 6. It is interesting to note here that the model satisfies the strong energy condition, which implies that the space-time does contain a black hole region.

The anisotropy, as expected, vanishes at the centre i.e., $p_{t\,eff} = p_{r\,eff} = p_{0\,eff} = \frac{2B-A}{8\pi}$ at $r=0$. The effective energy density and the two pressures are also well behaved in the interior of the stellar configuration.

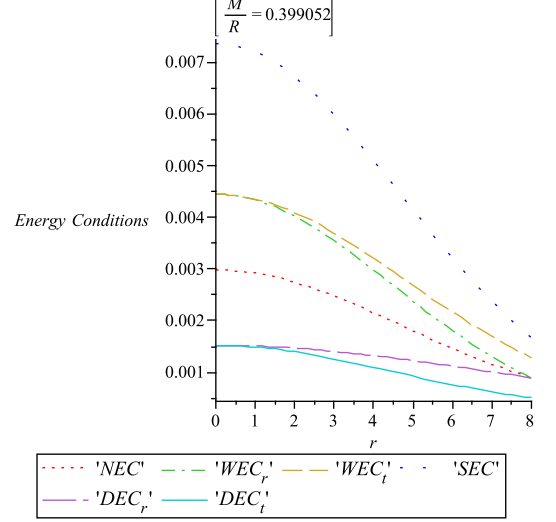


FIG. 6: The variation of left hand side of the expressions of energy conditions are shown against r .

Employing the energy conditions at the centre ($r = 0$), we may get a bound on the constants A and B as follows:

(i) NEC: $p_{0\,eff} + \rho_{0\,eff} \geq 0 \Rightarrow A + B \geq 0,$

(ii) WEC: $p_{0\,eff} + \rho_{0\,eff} \geq 0 \Rightarrow A + B \geq 0,$

$\rho_{0\,eff} \geq 0 \Rightarrow A \geq 0,$

(iii) SEC: $p_{0\,eff} + \rho_{0\,eff} \geq 0 \Rightarrow A + B \geq 0,$

$3p_{0\,eff} + \rho_{0\,eff} \geq 0 \Rightarrow B \geq 0,$

(iv) DEC: $\rho_{0\,eff} > |p_{0\,eff}| \Rightarrow 2A \geq B.$

VI. STABILITY

For a physically acceptable model, one expects that the velocity of sound should be within the range $0 \leq v_s = \left(\frac{dp}{d\rho}\right) \leq 1$ [20, 21]. In our anisotropic model, we define sound speeds as

$$v_{sr}^2 = \frac{dp_{r\,eff}}{d\rho_{eff}} = -1 + \frac{4A r e^{-Ar^2} (A + B)}{\left(2A - \frac{1}{r^2}\right) 2A r e^{-Ar^2} + \frac{2}{r^3} (1 - e^{-Ar^2})}, \quad (37)$$

$$v_{st}^2 = \frac{dp_{t\ eff}}{d\rho_{eff}} = \frac{e^{-Ar^2} [2Ar (B^2r^2 + 2B - ABr^2 - A) + 2Br(A - B)]}{(2A - \frac{1}{r^2}) 2Ae^{-Ar^2} + \frac{2}{r^3} (1 - e^{-Ar^2})}. \quad (38)$$

We plot the radial and transverse sound speeds in Fig. 7 and observe that these parameters satisfy the inequalities $0 \leq v_{sr}^2 \leq 1$ and $0 \leq v_{st}^2 \leq 1$ everywhere within the stellar object.

Equations (37) and (38) lead to

$$v_{st}^2 - v_{sr}^2 = 1 - \frac{e^{-Ar^2} [2A^2Br^3 + 6A^2r + 2Br^2 - 2ABr - 2AB^2r^3]}{(2A - \frac{1}{r^2}) 2Ae^{-Ar^2} + \frac{2}{r^3} (1 - e^{-Ar^2})}. \quad (39)$$

From equation (39), we note that $v_{st}^2 - v_{sr}^2 \leq 1$. Since, $0 \leq v_{sr}^2 \leq 1$ and $0 \leq v_{st}^2 \leq 1$, therefore, $|v_{st}^2 - v_{sr}^2| \leq 1$. In Fig. 8, we have plotted $|v_{st}^2 - v_{sr}^2|$.

Now, to examine the stability of local anisotropic matter distribution, we use Herrera's [20] cracking (or overturning) concept which states that the region for which radial speed of sound is greater than the transverse speed of sound is a potentially stable region. Thus, if the difference of the two sound speeds $v_{st}^2 - v_{sr}^2$ retains the same sign everywhere within a matter distribution, no cracking will occur. In our case, Fig. 9 indicates that there is no change of sign for the term $v_{st}^2 - v_{sr}^2$ within the specific configuration since the difference is negative throughout the distribution. Therefore, we conclude that our dark energy star model is stable.

VII. MASS-RADIUS RELATION

In this section, we study the maximum allowable mass-radius ratio in our model. For a static spherically symmetric perfect fluid star, Buchdahl [18] showed that the maximally allowable mass-radius ratio is given by $\frac{2M}{R} < \frac{8}{9}$ (for a more generalized expression for the same see Ref. [22]). In our model, the effective gravitational mass in terms of the effective energy density ρ_{eff} can be expressed as

$$M_{eff} = 4\pi \int_0^R (\rho + \rho_{de}) r^2 dr = \frac{1}{2}R (1 - e^{-AR^2}). \quad (40)$$

In Fig. 10, we plot this mass-radius relation. We have also plotted $\frac{M_{eff}}{R}$ against R (see Fig. 11) which shows that the ratio $\frac{M_{eff}}{R}$ is an increasing function of the radial parameter. We note that a constraint on the maximum allowed mass-radius ratio in our case is similar to the

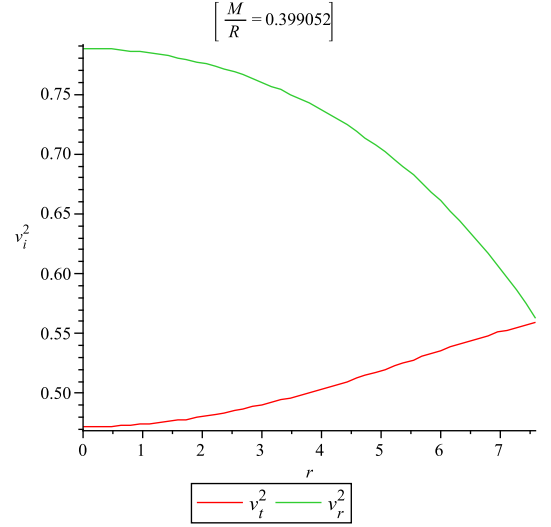


FIG. 7: The variation of radial sound speed v_{sr}^2 and tangential sound speed v_{st}^2 are shown against r .

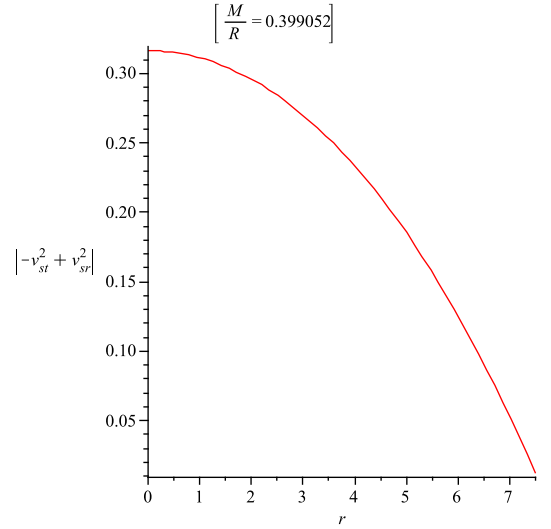


FIG. 8: The variation of $|v_{st}^2 - v_{sr}^2|$ is shown against r .

isotropic fluid sphere, i.e., $\frac{M}{R} < \frac{4}{9}$ as obtained earlier. The compactness of the star is given by

$$u = \frac{M_{eff}(R)}{R} = \frac{1}{2} (1 - e^{-AR^2}). \quad (41)$$

The surface redshift (Z_s) corresponding to the above compactness (u) is obtained as

$$Z_s = (1 - 2u)^{-\frac{1}{2}} - 1, \quad (42)$$

where

$$Z_s = e^{\frac{4}{2}R^2}. \quad (43)$$

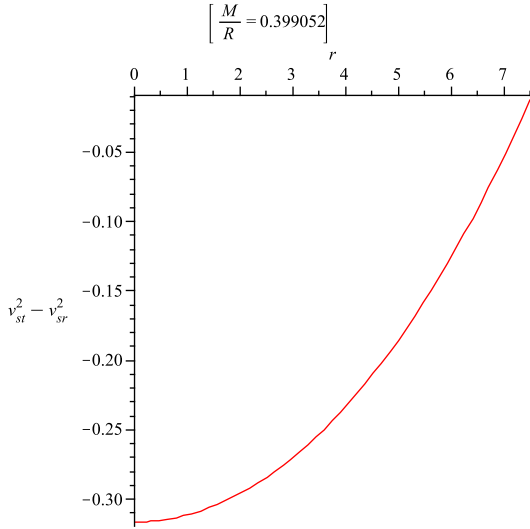


FIG. 9: The variation of $v_{st}^2 - v_{sr}^2$ is shown against r .

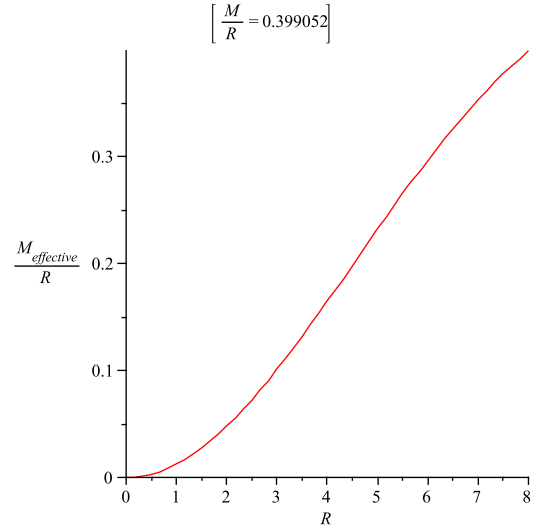


FIG. 11: The variation of $\frac{M_{effective}}{R}$ is shown against R .

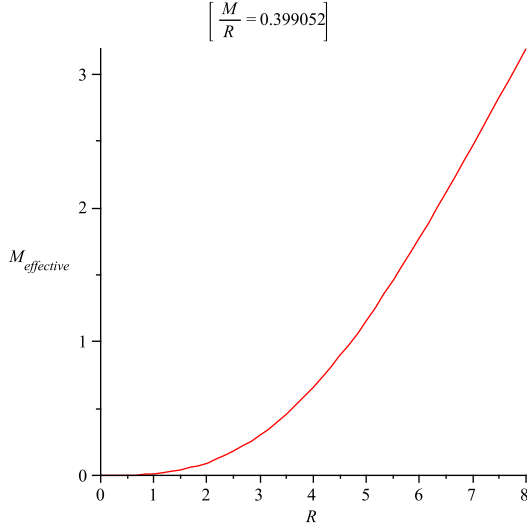


FIG. 10: The variation of $M_{effective}$ is shown against R .

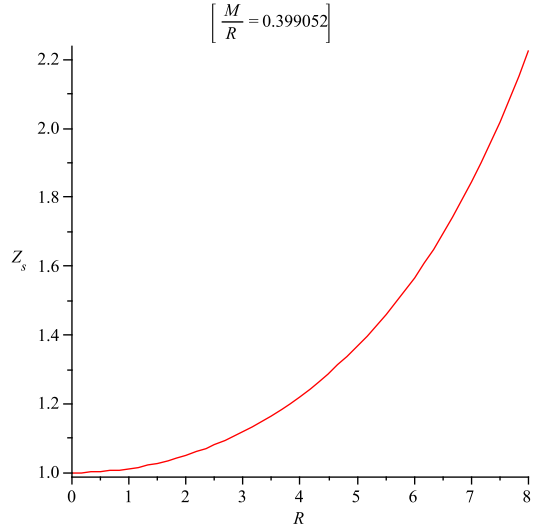


FIG. 12: The variation of redshift function Z_s is shown against R .

Thus, the maximum surface redshift for an anisotropic star of radius 8 km turns out to be $Z_s = 2.225541$.

VIII. JUNCTION CONDITION

One of the issues in connection with a static anisotropic matter distribution is that, though the radial pressure at the boundary of the star must vanish, the tangential pressure is not necessarily zero at the boundary. This forces us to examine the junction conditions of a static anisotropic star in closer details. We propose here a shell type envelope at the boundary surface so as to address

this issue. Note that the fundamental junction condition for a static star is that there has to be a smooth matching between the interior solution and Schwarzschild exterior at the boundary. Now, though the metric coefficients must be continuous at the junction surface S where $r = R$, their derivatives may not be continuous at the junction. In other words, the affine connections may be discontinuous at the boundary surface. This can be taken care of if we consider the second fundamental forms of the boundary shell. The second fundamental forms associated with the two sides of the shell [23–26]

are given by

$$K_{ij}^{\pm} = -n_{\nu}^{\pm} \left[\frac{\partial^2 X_{\nu}}{\partial \xi^i \partial \xi^j} + \Gamma_{\alpha\beta}^{\nu} \frac{\partial X^{\alpha}}{\partial \xi^i} \frac{\partial X^{\beta}}{\partial \xi^j} \right]_{|S}, \quad (44)$$

where n_{ν}^{\pm} are the unit normals to S and can be written as

$$n_{\nu}^{\pm} = \pm \left| g^{\alpha\beta} \frac{\partial f}{\partial X^{\alpha}} \frac{\partial f}{\partial X^{\beta}} \right|^{-\frac{1}{2}} \frac{\partial f}{\partial X^{\nu}}, \quad (45)$$

with $n^{\mu}n_{\mu} = 1$. In Eq. (45), ξ^i are the intrinsic coordinates on the shell with $f = 0$ being the parametric equation of the shell S and $-$ and $+$ correspond to interior and exterior (Schwarzschild) metrics. Note that radial pressure on the shell is zero. By using Lanczos equations [23–26], the surface energy term Σ and surface tangential pressures $p_{\theta} = p_{\phi} \equiv p_t$ may be obtained as

$$\Sigma = -\frac{1}{4\pi R} \left[\sqrt{e^{-\lambda}} \right]_{-}^{+}, \quad (46)$$

$$p_t = \frac{1}{8\pi R} \left[\left(1 + \frac{R\nu'}{2} \right) \sqrt{e^{-\lambda}} \right]_{-}^{+}. \quad (47)$$

Since the metric functions are continuous on S , we have

$$\Sigma = 0, \quad (48)$$

and

$$p_t = \frac{1}{8\pi R} \left[\frac{\left(\frac{M}{R} \right)}{\sqrt{1 - \frac{2M}{R}}} - BR^2 \sqrt{e^{-AR^2}} \right]. \quad (49)$$

Therefore, we are now in a position to match our interior solution to the Schwarzschild exterior in the presence of a thin shell.

From Fig. 13, we note that the effective transverse pressure at the boundary ($R = 8$ km) is positive though the transverse pressure in the shell is negative. This clearly indicates that the static equilibrium may be attained due to positive $p_{t \text{ eff}}$ and negative $p_{t \text{ shell}}$. In this figure, we have plotted $p_{t \text{ eff}}$ and $p_{t \text{ shell}}$ together by assuming that the width of the shell is in between 8 – 15 km. We observe that at $r = 15$ km, both $p_{t \text{ eff}}$ and $p_{t \text{ shell}}$ vanish simultaneously. Thus the thickness of the shell in this case is 7 km. Physically, this suggests that anisotropic matter is confined within 8 km from the centre of the star and the outer region contains a thick shell extending up to 7 km. The thick shell is characterized by zero energy density and non zero transverse pressure though the shell does not exert any radial pressure.

IX. CONCLUSION

Dark energy stellar models have found astrophysical relevance for various reasons, one particular reason being its importance as an alternative candidate to a black

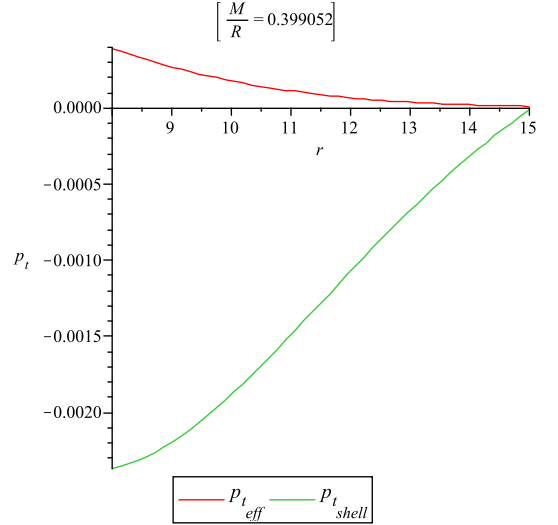


FIG. 13: Plot for $p_{t \text{ eff}}$ and $p_{t \text{ shell}}$ is shown against r .

hole. The model developed here satisfies all the physical requirements and is horizon free and, therefore, can potentially describe a compact object which is neither a neutron star nor a quark star.

Similar to many models proposed earlier, our model also requires an envelope just outside the baryonic matter for smooth matching with the Schwarzschild exterior spacetime. For matching we have *firstly*, assumed continuity of the metric functions g_{tt} , g_{rr} and $\frac{\partial g_{tt}}{\partial r}$ at the boundary surface S , and *secondly* imposed the boundary conditions that at the boundary $(p_r)_{\text{eff}}(r = R) = 0$ and $\rho_{\text{eff}}(r = 0) = b$ ($= a$ constant), where b is the central density. Thus we get a set of expressions for A , B and C which, due to the maximum allowable compactness for a fluid sphere [18], eventually can be worked out as $A = .025$, $B = .030883$, $b = .002984$ for the assumed mass-radius ratio as $\frac{M}{R} = 0.399052$. Later on, in Sec. V, it has been shown that these values of A and B are justified since the energy conditions imply $2A \geq B \geq 0$.

Regarding stability of local anisotropic matter distribution, we use the cracking concept of Herrera [20] which states that the region for which radial speed of sound is greater than the transverse speed of sound is a potentially stable region. It is observed from Fig. 9 that there is no change of sign for the term $v_{st}^2 - v_{sr}^2$ within the specific configuration and hence advocating in favour of stability of our dark energy star model.

Let us now concentrate on some of the other works on KB analysis, especially the works by Varela et al. [27] and Farook et al. [28]. In both the works static, spherically symmetric, Einstein-Maxwell spacetime have been considered with a fluid source of anisotropic stresses whereas the present investigation is neutral one with anisotropic fluid source. However, a common feature of all these KB-models is singularity-free, stable configurations. Valera

et al.[27] in their work have found out a link of their construction with a charged strange quark star as well as models of dark matter including massive charged particles. Farook et al.[28], by using a Chaplygin-type EOS, predicted the possible existence of a Chaplygin charged dark energy star or a strange quark star of radius about 8 km.

Therefore, it is interesting to note that present work deals with a singularity-free spherically symmetric body of radius $r = 15$ km such that both $p_{t\,eff}$ and $p_{t\,shell}$ vanish simultaneously. The model physically contains anisotropic matter which is confined within 8 km from the centre of the star and the outer region contains a thick shell extending up to 7 km. Here the thick shell is characterized by zero energy density and non-zero transverse pressure though the shell does not exert any radial pressure. Note that in a recently proposed toy model [29], a relativistic stellar configuration has been developed where the core of the star is characterized by a wormhole like solution for some kind of exotic matter violating the weak/null energy condition and is surrounded

by some ordinary matter satisfying a polytropic EOS. This kind of theoretical modelling would get observational support in the future.

We hope our model inspires observational workers to search this type of stars. That is, we mean, the stars containing anisotropic matter which is confined within certain radius from the centre of the star and the outer region contains a thick shell extending up to several kilometer.

Acknowledgments

FR, SR and RS gratefully acknowledge support from IUCAA, Pune, India under Visiting Associateship under which a part of this work was carried out. FR is also thankful to PURSE for providing financial support. We thank the anonymous referee for drawing our attention to a couple of references relevant to our studies.

-
- [1] S. Perlmutter *et al*, Nature **391**, 51 (1998).
 - [2] A. G. Riess *et al*, Astrophys. J. **607**, 665 (2004).
 - [3] M. A. Abramowicz, W. Kluzniak and J. P. Lasota, Astron. Astrophys. **396**, L31 (2002).
 - [4] F. S. N. Lobo, Class. Quantum Grav. **23**, 1525 (2006), **24**, 1069 (2007).
 - [5] G. Chapline, Proceedings of the Texas Conference on Relativistic Astrophysics, Stanford, CA, December, (2004).
 - [6] P. O. Mazur and E. Mottola, arXiv:gr-qc/0109035.
 - [7] R. Chan, M. F. A. da Silva and J. F. V. da Rocha, Gen. Relativ. Gravit. **41**, 1835 (2009).
 - [8] C. R. Ghezzi, Phys. Rev. D **72** 104017 (2005).
 - [9] T. Padmanabhan, Gen. Relativ. Gravit. **40**, 529 (2008).
 - [10] R. L. Bowers and E. P. T. Liang, Astrophys. J., **188**, 657 (1974).
 - [11] L. Herrera and N. O. Santos, Astrophys. J., **438**, 308 (1995).
 - [12] Stoytcho S. Yazadjie, arXiv:1104.1865v2 [gr-qc].
 - [13] K. D. Krori and J. Barua, J. Phys. A.: Math. Gen. **8**, 508 (1975).
 - [14] C. W. Davies, Phys. Rev. **D30**, 737 (1984).
 - [15] J. J. Blome and W. Priester, Naturwissenschaften **71**, 528 (1984).
 - [16] C. Hogan, Nature **310**, 365 (1984).
 - [17] N. Kaiser and A. Stebbins, Nature **310**, 391 (1984).
 - [18] H. A. Buchdahl, Phys. Rev. **116**, 1027 (1959).
 - [19] J. Ponce de León, Gen. Relativ. Gravit. **25**, 1123 (1993).
 - [20] L. Herrera, Phys. Lett. A, **165** 206, (1992).
 - [21] H. Abreu, H. Hernandez and L. A. Nunez, Class. Quantum Gravit. **24**, 4631 (2007).
 - [22] M. K. Mak, P. N. Dobson and T. Harko, Europhys. Lett. **55**, 310 (2001).
 - [23] W. Israel, Nuo. Cim. B **44**, 1 (1966); erratum - ibid. **48B**, 463 (1967).
 - [24] A. A. Usmani, Z. Hasan, F. Rahaman, Sk. A. Rakib, S. Ray, P. K. F. Kuhfittig, Gen. Relativ. Gravit. **42**, 2901 (2010).
 - [25] F. Rahaman, K. A. Rahman, Sk. A. Rakib, P. K. F. Kuhfittig, Int. J. Theor. Phys. **49**, 2364 (2010).
 - [26] F. Rahaman, P. K. F. Kuhfittig, M. Kalam, A. A. Usmani and S. Ray, arXiv:gr-qc/1011.3600.
 - [27] V. Varela, F. Rahaman, S. Ray, K. Chakraborty and M. Kalam, Phys. Rev. D **82**, 044052 (2010).
 - [28] F. Rahaman, S. Ray, A. K. Jafry and K. Chakraborty, Phys. Rev. D **82**, 104055 (2010).
 - [29] Vladimir Dzhunushaliev et al, arXiv:1102.4454v3 [astro-ph.GA]